The FEBS Journal

FEBS PRESS science publishing by scientists

ISL1 regulates the differentiation and maintenance of dental epithelial stem cells in the incisor

Yaping Qu, Huizhou Liu, Yan Wang, Shanhui Gao, Huarong Huang, Jianying Li, Mengsheng Qiu and Feixue Li

Zhejiang Key Laboratory of Organ Development and Regeneration, College of Life and Environmental Sciences, Hangzhou Normal University, People's Republic of China

Keywords
ameloblast; ISL1; Sox2; stem cell; tooth

Correspondence
F. Li, Zhejiang Key Laboratory of Organ Development and Regeneration, College of Life and Environmental Sciences, Hangzhou Normal University, Hangzhou 310036, People's Republic of China
Tel: +86 571 28865657
E-mail: lifx@hznu.edu.cn

Yaping Qu and Huizhou Liu contributed equally to this work

(Received 5 June 2025, revised 28 June 2026, accepted 18 August 2026)

doi:10.1111/febs.70713

Enamel is asymmetrically distributed in mouse incisors, which grow throughout life, and this continuous renewal is driven by dental epithelial stem cells (DESCs). In this study, we report that ablation of *Isl1* in the dental epithelium using Pitx2-Cre leads to impaired development of the mandibular incisors. In $Isl1^{Pitx2Cre}$ mutant embryos, the mandibular incisors exhibited a significant reduction in size and length compared to wild-type controls. A significant decrease in the proliferation of epithelial and mesenchymal cells was also detected in $Isl1^{Pitx2Cre}$ mutant incisors, and cell apoptosis was markedly increased in the lateral cervical loop of $Isl1^{Pitx2Cre}$ mutant incisors at E17.5. Ameloblasts and enamel were present on all surfaces of the mandibular incisor, including the labial side. Transcriptome analysis and in situ hybridisation revealed that *Isl1* deletion induced significant upregulation of Hedgehog pathway components (*Shh*, *Ptch1*, *Gli1*) and FGF signalling mediators (*Fgf3*, *Etv4*, *Etv5*), while downregulating dental epithelial stem cell markers *Sox2* and *Lgr5*. Our results showed that ISL1 co-localised with SOX2 in the lingual and lateral dental epithelium of mandibular incisors, and the expression of *Sox2* was regulated by *Isl1*. Our results demonstrate that *Isl1* sustains DESC viability and orchestrates ameloblast lineage commitment via SOX2-mediated regulation during incisor morphogenesis.

Introduction

Enamel is the only calcified tissue in mammalian epithelial cells and the hardest tissue in the human body. Tooth enamel is asymmetrically distributed in mouse incisors, where the enamel covers only the labial side. This asymmetry favours abrasion on the lingual side, resulting in sharp incisor edges on the labial side. The presence of dental epithelial stem cells (DESCs) allows the abrasion of the incisors to be compensated by continuous growth [1]. The regulation of stem cell renewal and differentiation is a complex regulatory network, including the interaction between signalling pathways such as WNT, FGF, BMP, NOTCH and Hedgehog [2–8].

Tooth development experiences a dental lamina stage, bud stage, Cap stage, bell stage and secretory stage [8,9]. The lingual cervical loop (liCL) and lateral cervical loop (laCL) begin to form in the bell period, and they both contain DESCs [10]. The self-renewal and differentiation of DESCs are regulated by multiple regulatory signals [11]. *Sox2* marks DESCs and is

Abbreviations
BrdU, bromodeoxyuridine; ChIP, chromatin immunoprecipitation; DESCs, dental epithelial stem cells; EGTA, ethylene glycol tetraacetic acid; ISL1, insulin gene enhancer binding protein 1; laCL, lateral cervical loop; liCL, lingual cervical loop; MMRRC, Mutant Mouse Resource and Research Center; OEE, outer enamel epithelium; PFA, paraformaldehyde; RNA-Seq, RNA sequencing; SR, stellate reticulum; TUNEL, terminal deoxynucleotidyl transferase (TdT) dUTP nick-end labelling.

essential for the maintenance of the DESCs in adult mice [12]. Ablation of *Sox2* in the dental epithelium results in mandibular incisor development arrest and impaired DESCs proliferation [13]. SHH and FGF signalling also play important roles in regulating the development and function of ameloblasts [14–17]. Conditional knockout of *Smo* or *Shh* in dental epithelial cells leads to defects in cell proliferation and ameloblast development [18,19]. *Fgf3* knockout mice have defects in enamel formation. Furthermore, *Fgf3* and *Fgf10* double knockout mice have very thin or missing enamel [7]. Deletion of FGF3 and FGF10 receptor FGFR2 resulted in a significant reduction in tooth epithelial cell proliferation and cessation of tooth development before the bud stage [20].

Insulin gene enhancer binding protein 1 (ISL1) is a LIM homeodomain transcription factor and is essential for many developmental processes [21–25]. ISL1 also marks cardiovascular progenitors and endothelial cell lineages [26,27]. Recently, *Isl1* was reported to be important for patterning of enamel in the incisor [28]. Ectopic enamel on the lingual surface of incisors was observed in $Isl1^{K14Cre}$ mice. Considering that tooth development begins around E9.5-E10.5 in mouse, we knocked out *Isl1* using Pitx2-Cre mice. Pitx2-Cre mice expressed CRE at E10.5, earlier than Krt14-Cre mice expressing CRE at E11.75 [29]. Our data confirmed that *Isl1* is critical for the enamel asymmetry in the incisor, which is consistent with previous data. In addition, we found that *Isl1* is essential for incisor epithelial cell proliferation and maintenance of DESCs. This study is the first to demonstrate that ISL1 plays a dual role in maintaining dental epithelial stem cells (DESCs) and regulating ameloblast patterning.

Results

Ablation of Isl1 changed enamel pattern and disrupts incisor development

The expression of *Isl1* during tooth development was analysed using the $Isl1^{LacZ}$ allele. *Isl1* expression was detected in the mandible epithelium as early as E10.5 (Fig. 1A). *Isl1* was expressed on the labial and lingual sides of the incisor at E14.5 and E15.5 (Fig. 1A). *Isl1* expression on the lingual side increased significantly at

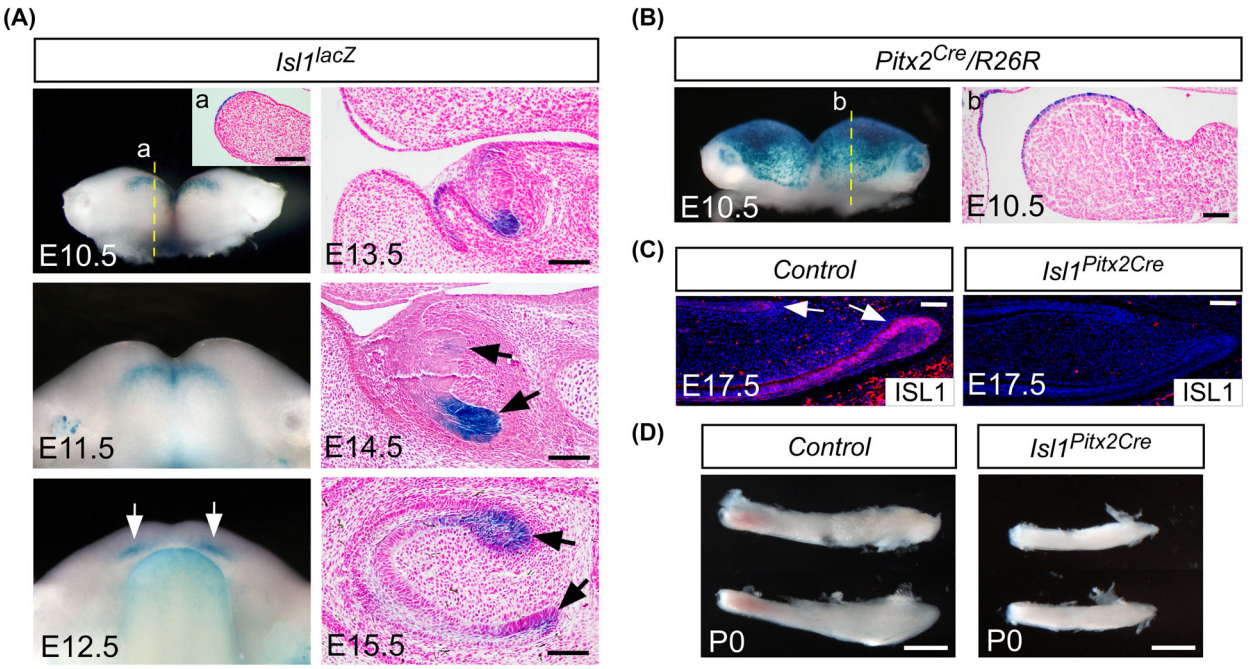

Fig. 1. Dental epithelial inactivation of *Isl1* leads to incisor development defects. (A) X-Gal staining shows *Isl1* expression in $Isl1^{LacZ}$ knock-in mice at E10.5-E15.5 (arrows) ($n = 3$). Yellow dashed line indicates approximate section levels crossing the mandible. Inset shows haematoxylin and eosin staining on sagittal sections. (B) X-Gal staining shows Pitx2-Cre activity in $Pitx2^{Cre}/R26R$ mice at E10.5 ($n = 3$). Yellow dashed line indicates approximate section levels crossing the mandible. Right: X-Gal staining shows Pitx2-Cre activity in E10.5 $Pitx2^{Cre}/R26R$ mandibular arch. (C) Immunofluorescence demonstrates ISL1 expression in the $Pitx2^{Cre}$ (control) and $Isl1^{Pitx2Cre}$ palates at E17.5 (arrows) ($n = 3$). (D) Incisors of control ($Pitx2^{Cre}$) and $Isl1^{Pitx2Cre}$ at P0 ($n = 4$). E, embryonic day; P, postnatal day; scale bars: 100 μm (B, C), 200 μm (Aa), 500 μm (D).

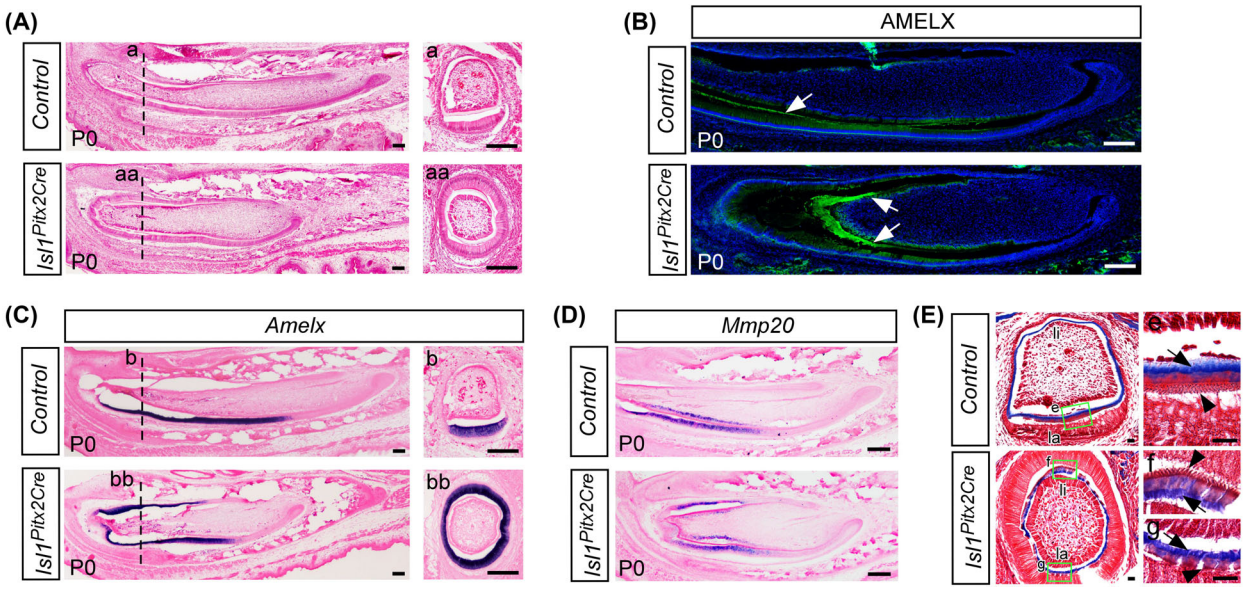

Fig. 2. Dental epithelial inactivation of *Isl1* leads to ameloblast pattern defects. (A) Sagittal and cross-sectional views show ectopic ameloblast on the lingual side of mutant ($Isl1^{Pitx2Cre}$) but not control ($Pitx2^{Cre}$) incisors at P0 ($n = 5$). Black dashed line indicates approximate section levels crossing the incisor. (B) Immunofluorescence shows ectopic AMELX on the lingual side of mutant ($Isl1^{Pitx2Cre}$) but not control ($Pitx2^{Cre}$) incisors at P0 (arrows) ($n = 3$). (C) In situ hybridisation shows ectopic *Amelx* on the lingual side of mutant ($Isl1^{Pitx2Cre}$) but not control ($Pitx2^{Cre}$) incisors at P0 ($n = 3$). Black dashed line indicates approximate section levels crossing the incisor. (D) In situ hybridisation shows ectopic *Mmp20* on the lingual side of mutant ($Isl1^{Pitx2Cre}$) but not control ($Pitx2^{Cre}$) incisors at P0 ($n = 3$). (E) Masson's trichrome staining of control and mutant incisors at P0. Black arrowheads show the enamel matrix (red) ($n = 3$). Black arrows show the dentin (blue). P, postnatal day; li, lingual side; la, labial side. Scale bars: 200 μm (A–D), 20 μm (E).

E15.5 (Fig. 1A). To explore the role of *Isl1* in incisor development, ISL1 was specifically removed from dental epithelial cells with $Pitx2^{Cre}$ mice. $Pitx2^{Cre}$ mice exhibited Cre activities in the mandible epithelium at E10.5 (Fig. 1B). Immunohistochemical analysis showed that there is no ISL1 protein in the incisors of the mutant mice ($Isl1^{Pitx2Cre}$) at E17.5 (Fig. 1C, Control). Both male and female Mice heterozygous for the *Isl1* mutation were normal and fertile. The mutant alleles ($Isl1^{Pitx2Cre}$) were born normally according to the Mendelian ratio but died at postnatal day 0 (P0). The mandibular incisors of $Isl1^{Pitx2Cre}$ mutant embryos showed as significantly smaller and shorter than those of wild type (100% penetration) (Fig. 1D). The results suggest that *Isl1* gene deletion leads to the defect of mandibular incisors development.

We analysed the mandibular incisor phenotype in the new born *Isl1* mutant embryos. Surprisingly, a well-polarised layer of cells was present not only on the labial surface of the incisor but on all surfaces (Fig. 2A). Both enamel matrix protein amelogenin (AMELX) and MMP20 play important roles in enamel formation [30]. In situ hybridisation and immunostaining showed that both AMELX and MMP20 were expressed in the well-polarised cells, suggesting that the well-polarised cells were ameloblasts (Fig. 2B–D). Masson's trichrome staining enables differentiation between enamel matrix (stained red) and dentin/bone (stained blue). In the mutant incisors, enamel matrix was observed not only on the labial side but across the entire surface of the incisor (Fig. 2E). Compared to the wild type, the mutant shows irregularly arranged enamel rods (Fig. 2E). These findings indicate that ISL1 is required for both correct ameloblast patterning and the orderly organisation of enamel rods in the incisor.

Isl1 deletion leads to the change of cell proliferation and apoptosis in a cervical loop

In order to explore the cellular mechanism of the *Isl1* mutant incisor development defect, the cell proliferation and apoptosis were studied. Bromodeoxyuridine (BrdU) labelling was used to assess the proliferating cells. At E14.5 and E15.5, the results showed that the BrdU-labelled epithelial and mesenchymal cells in *Isl1* mutant ($Isl1^{Pitx2Cre}$) incisors were significantly reduced (Fig. 3A–C). At E17.5, the number of proliferating cells increased in the liCL side and decreased in the laCL side of the mutant incisors (Fig. 3A,D). Terminal

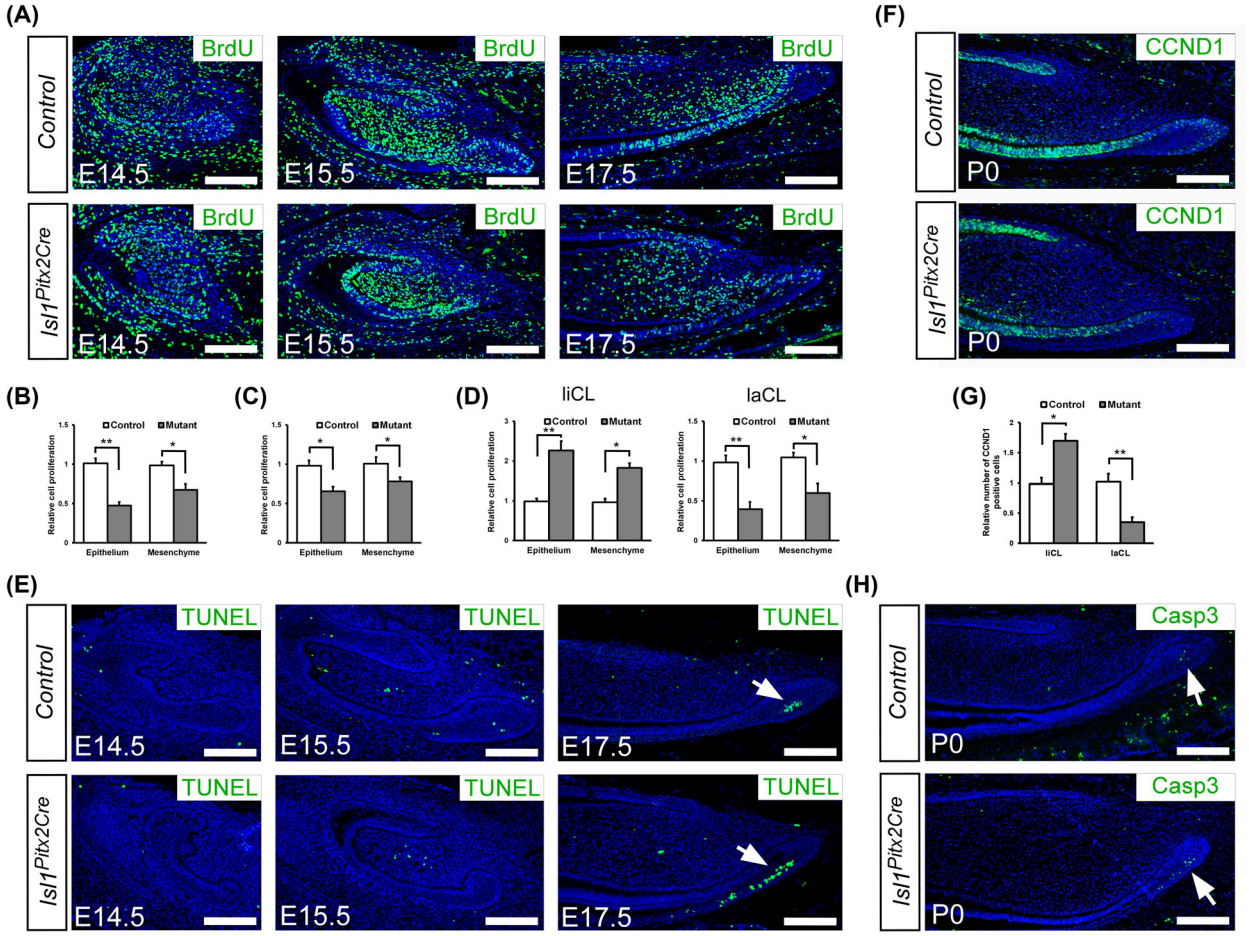

Fig. 3. Deletion of Isl1 in dental epithelial cells results in defects of cell proliferation and apoptosis in the mandibular incisors. (A) BrdU labelling assays show the cell proliferation in the incisors of $Isl1^{Pitx2Cre}$ embryo and control ($Pitx2^{Cre}$) ($n = 4$). (B) Comparison of epithelial and mesenchymal cell proliferation in the incisors between control ($Pitx2^{Cre}$) and mutant ($Isl1^{Pitx2Cre}$) at E14.5. Error bars represent SEM ($n = 4$; Student's *t*-test). (C) Comparison of epithelial and mesenchymal cell proliferation in the incisors between control ($Pitx2^{Cre}$) and mutant ($Isl1^{Pitx2Cre}$) at E15.5. Error bars represent SEM ($n = 4$; Student's *t*-test). (D) Comparison of relative proliferation in the liCL and laCL between control ($Pitx2^{Cre}$) and mutant ($Isl1^{Pitx2Cre}$) at E17.5. Error bars represent SEM ($n = 4$; Student's *t*-test). (E) TUNEL staining shows cell apoptosis in the mandibular incisors of $Isl1^{Pitx2Cre}$ and control ($Pitx2^{Cre}$) (arrows) ($n = 3$). (F) CCND1 immunofluorescence staining in the incisors of $Isl1^{Pitx2Cre}$ embryo and control ($Pitx2^{Cre}$) at P0 ($n = 3$). (G) Comparison of the relative number of CCND1 positive cells in the liCL and laCL between control ($Pitx2^{Cre}$) and mutant ($Isl1^{Pitx2Cre}$) at P0. Error bars represent SEM ($n = 3$; Student's *t*-test). (H) Active Caspase-3 (Casp3) immunofluorescence staining in the incisors of $Isl1^{Pitx2Cre}$ embryo and control ($Pitx2^{Cre}$) at P0 (arrows) ($n = 3$). E, embryonic day; P, postnatal day; liCL, lingual cervical loop; laCL, lateral cervical loop; *, $P < 0.05$. **, $P < 0.01$. Scale bars: 200 μm.

deoxynucleotidyl transferase dUTP nick-end labelling (TUNEL) assay was performed to detect the cell apoptosis. There was no significant difference in apoptosis between the wild-type ($Pitx2^{Cre}$) and $Isl1^{Pitx2Cre}$ incisors at E14.5 and E15.5 (Fig. 3E). In the mutant laCL, the number of apoptotic cells in the stellate reticulum near the outer enamel epithelium was significantly increased at E17.5 (Fig. 3E).

We performed immunofluorescence staining for CCND1 (cell cycle regulator) and active Caspase-3 (apoptosis marker) on P0 sections (Fig. 3F–H). Specifically, the liCL region in the mutant incisors shows higher CCND1 signal, consistent with active proliferation. In contrast, the laCL region in the mutant incisors exhibits elevated active Caspase-3 and reduced CCND1 expression. The differential expression of CCND1 and active Caspase-3 may contribute to the differential proliferative activity observed between the liCL and laCL in the mutant incisors.

Isl1 is required for DESCs maintenance

To gain insight into the molecular mechanism by which *Isl1* deletion causes defects in incisor development, we

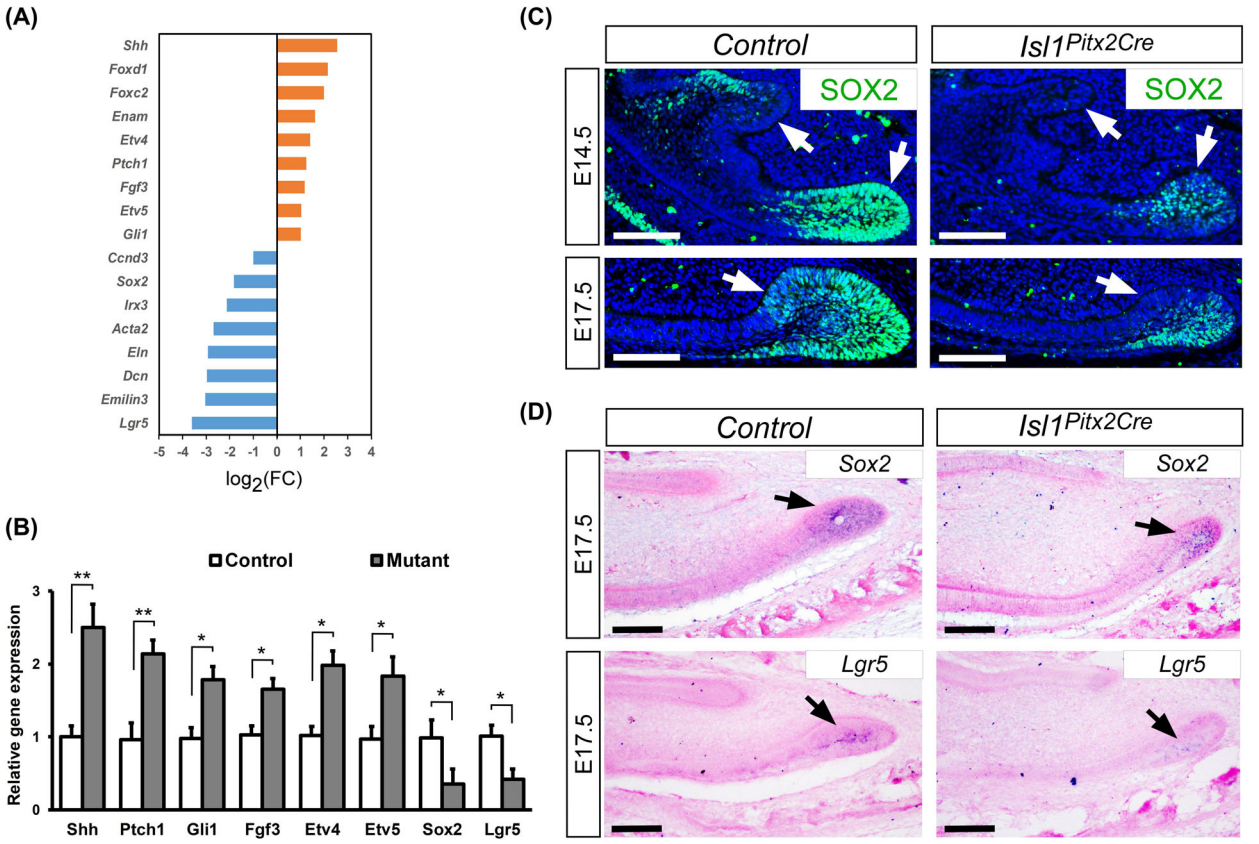

Fig. 4. Differentially expressed genes in the mutant mandibular incisors. (A) Representative examples of differentially expressed genes in the *Isl1*^{Pitx2Cre} as revealed by RNA-Seq analysis (≥ 2-fold, < 5% false discovery rate). (B) Quantitative RT-PCR demonstrates transcription of *Shh*, *Ptch1*, *Gli1*, *Fgf3*, *Etv4*, *Etv5*, *Sox2* and *Lgr5* in the incisors of control (*Pitx2*^{Cre}) and *Isl1*^{Pitx2Cre} at E14.5. Error bars represent SEM (n = 4; Student's t-test). (C) Immunofluorescence shows the expression of SOX2 in the incisors of *Pitx2*^{Cre} (control) and *Isl1*^{Pitx2Cre} at E14.5 and E17.5 (arrows) (n = 3). (D) In situ hybridisation shows the expression of *Sox2* and *Lgr5* in the incisors of control (*Pitx2*^{Cre}) and *Isl1*^{Pitx2Cre} at E17.5 (arrows) (n = 3). E, embryonic day; *, $P < 0.05$. **, $P < 0.01$. Scale bars: 100 μm.

analysed gene expression profiles of E14.5 mandibular incisors of mutant (*Isl1*^{Pitx2Cre}) and control (*Pitx2*^{Cre}) embryos using RNA-Seq. In parallel comparison, we identified dozens of protein-coding genes that showed differential expression between the mutants and the control (≥ 2 fold, < 5% false discovery rate; Fig. 4A). Quantitative real-time PCR (qRT-PCR) using RNAs purified from independent samples confirmed the altered expression of *Shh*, *Ptch1*, *Gli1*, *Fgf3*, *Etv4*, *Etv5*, *Sox2* and *Lgr5* (Fig. 4B). Among them, *Sox2* and *Lgr5* —known to be the markers for DESCs—significantly decreased [12,31]. *Sox2* has been reported to control ameloblast lineage commitment and its asymmetric patterning in mouse incisor [32]. Our immunostaining and in situ hybridisation analyses verified the decreased expression of *Sox2* and *Lgr5* in mutant incisor cervical loops at E14.5 and E17.5 (Fig. 4C,D). In particular, SOX2 expression was absent in the lingual dental epithelium of mutant embryos at E14.5 (Fig. 4C). The absence of SOX2^{+} DESCs in the lingual cervical loop might account for the appearance of ameloblasts in the lingual dental epithelium. Given the critical role of SOX2 in the maintenance of DESCs, the reduction of SOX2 expression in the lateral dental epithelium may lead to the increase of apoptosis at E17.5 (Fig. 3C). *Trp63* and *Notch1* were also reported to be implicated in the maintenance of dental epithelial stem cells. The expression of *Trp63* (Fig. 5A–F) and *Notch1* (Fig. 5G, H) was downregulated in the incisors of the mutant at E14.5–E17.5. In addition, *Bmp4*, a regulator of dental epithelial differentiation, was also increased in both the lingual and lateral cervical loops of the mutant incisors (Fig. 5I,J).

At E13.5, E14.5 and E17.5, SOX2 and ISL1 were colocalised in the lingual and lateral dental epithelium of mandibular incisors (Fig. 6A,B). It is hypothesised that *Sox2* is a downstream target of ISL1. One ISL1 consensus binding site was identified in the *Sox2*

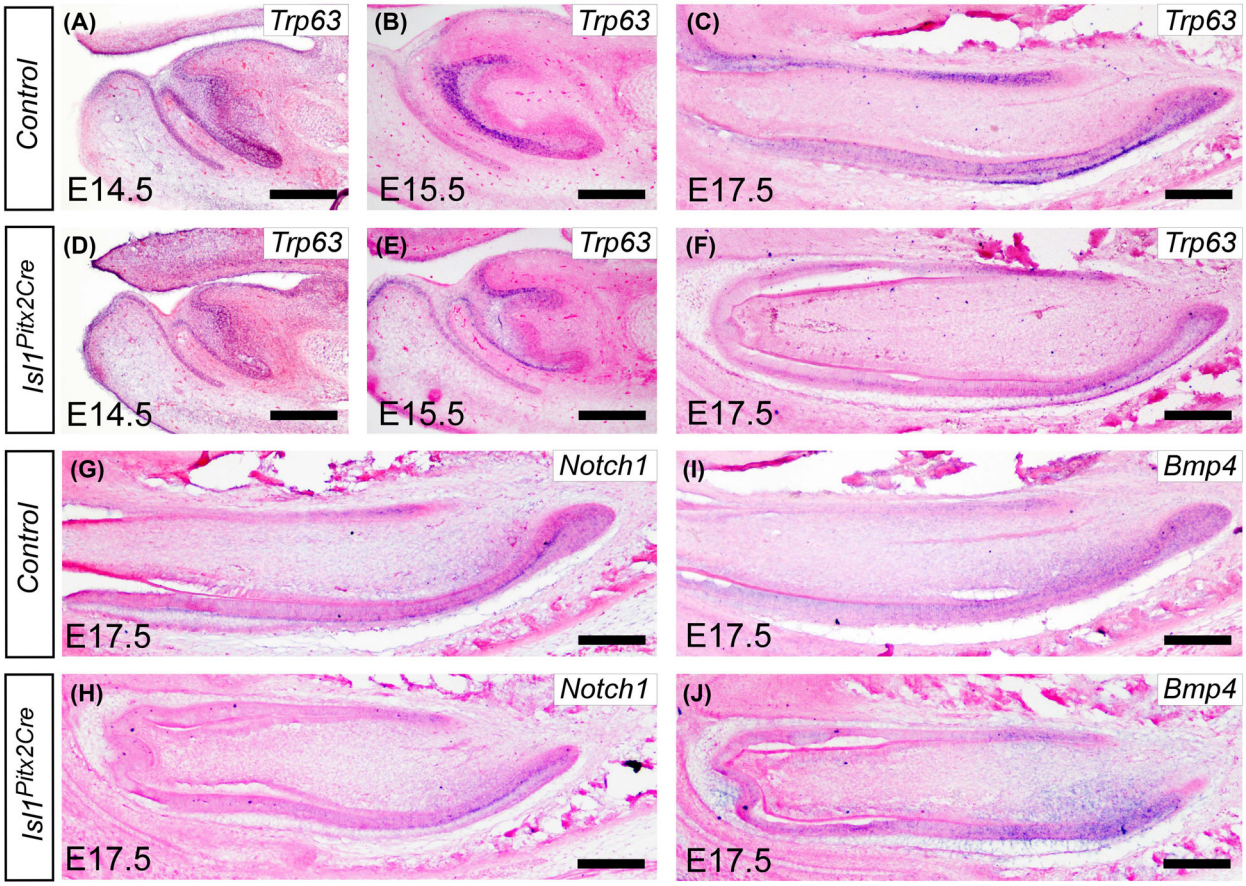

Fig. 5. Expression of *Trp63*, *Notch1* and *Bmp4* mRNA expression in the incisors of control ($Pitx2^{Cre}$) and $Isl1^{Pitx2Cre}$ at E14.5, E15.5 and E17.5. In situ hybridisation shows the expression of *Trp63* in the incisors of control ($Pitx2^{Cre}$) and $Isl1^{Pitx2Cre}$ at E14.5, E15.5 and E17.5 ($n = 3$). The expression of *Notch1* and *Bmp4* is also detected by in situ hybridisation in the incisors of control ($Pitx2^{Cre}$) and $Isl1^{Pitx2Cre}$ at E17.5 ($n = 3$). E, embryonic day; scale bars: 200 μm.

promoter sequence (Fig. 6C). ChIP analysis confirmed that ISL1 can bind to the site (Fig. 6D). Overexpression of *Isl1* significantly upregulated *Sox2* expression in mutant ($Isl1^{Pitx2Cre}$) incisors (Fig. 6E). Consistently, *Sox2* promoter activity was also stimulated by *Isl1* overexpression (Fig. 6F). Considering that $SOX2^{+}$ dental epithelial stem cells are important for postnatal incisor growth, we cultured P0 incisors from mutant and wild-type mice for five days. The mutant incisors did not change, whereas the wild-type incisors became longer (Fig. 6G). Together, these results indicate that *Sox2* is regulated by ISL1.

SHH, FGF and BMP signalling is upregulated in the lingual and lateral cervical loop of mutant incisors

It has been reported that *Sox2* can regulate the differentiation of dental epithelium by modulating SHH and FGF signalling [32]. The expression of *Shh*, *Ptch1*, *Fgf3* and *Etv5* were analysed in the mutant by in situ hybridisation. *Ptch1* and *Etv5* are marker genes of SHH signalling and FGF signalling activity, respectively. The results of in situ hybridisation showed that *Shh* expression was present in the lingual dental epithelium of the mutant, starting at E15.5, but not in the wild type (Fig. 7). The expression of *Etv5* was increased in the lingual dental epithelium of the mutant starting at E14.5 (Fig. 8). The expression of *Ptch1 and Fgf3* was increased in the mesenchyme of the mutant at E14.5 and E15.5 (Figs 7, 8). The expression of *Shh*, *Ptch1*, *Fgf3* and *Etv5* was also increased in the lateral cervical loop of the mutant incisors (Figs 7, 8). The results indicated that SHH, FGF and BMP signalling were upregulated not only in the lingual cervical loop but also in the lateral cervical loop of the mutant incisors (Figs 5, 7, 8). The upregulation of SHH, FGF and BMP signalling in the lingual

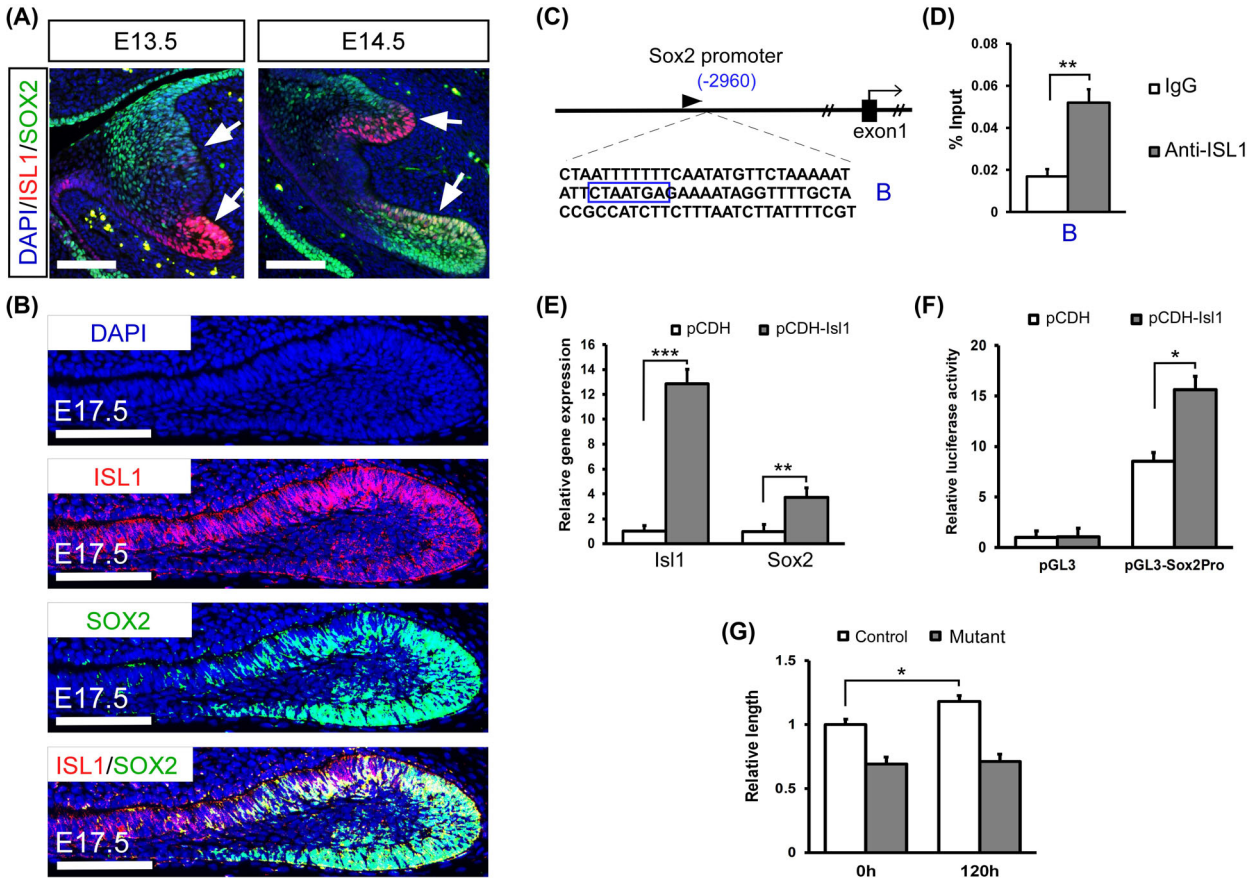

Fig. 6. ISL1 and SOX2 were colocalised in the liCL and laCL. (A) Immunofluorescence shows the colocalisation of ISL1 and SOX2 in the incisors at E13.5 and E14.5 (white arrows) ($n = 3$). (B) Immunofluorescence shows the colocalisation of ISL1 and SOX2 in the laCL of incisors at E17.5 ($n = 3$). (C) Schematic representation of the Sox2 promoter sequence. The binding site for ISL1 is highlighted 'B'. (D) Quantitative analysis of ChIP assays is performed by real-time PCR. Error bars represent SEM ($n = 3$; Student's *t*-test). (E) Quantitative RT-PCR demonstrates that overexpression of *Isl1* induced the expression of *Sox2* in the incisor cultures. Error bars represent SEM ($n = 4$; Student's *t*-test). (F) Luciferase activity of pGL3 empty vector (control) and pGL3-Sox2 promoter vector (pGL3-Sox2 Pro). Error bars represent SEM ($n = 4$; Student's *t*-test). (G) Relative length of incisors of control ($Pitx2^{Cre}$) and $Isl1^{Pitx2Cre}$. Error bars represent SEM ($n = 3$; Student's *t*-test). E, embryonic day; liCL, lingual cervical loop; laCL, lateral cervical loop; *, $P < 0.05$. **, $P < 0.01$. ***, $P < 0.001$. Scale bars: 100 μm.

cervical loop of the mutant incisors may induce the ectopic ameloblast differentiation. Taken together, *Isl1* deletion results in the upregulation of SHH, FGF, and BMP signalling pathways, thereby promoting ameloblast differentiation.

Discussion

Studies in animals and humans have identified many genes that play important roles in ameloblast patterning and differentiation [7,30,33,34]. In this study, abnormal enamel patterning was found in $Isl1^{Pitx2Cre}$ mutant embryos, indicating that *Isl1* is critical for the enamel asymmetry in the incisor. In addition, we provide evidence that *Isl1* is essential for the maintenance of DESCs.

The incisors of the mutant ($Isl1^{Pitx2Cre}$) were smaller and shorter than those of the wild type, which indicated that there were defects in the growth of mandibular incisors. Our results showed that the proliferation of epithelial and mesenchymal cells of *Isl1* mutant ($Isl1^{Pitx2Cre}$) incisors is significantly reduced at E14.5 and E15.5. A significant reduction in cell proliferation was also detected in the laCL of mutants at E17.5. In addition, the number of apoptotic cells in the stellate reticulum (SR) of laCL was increased in the mutants at E17.5. DESCs reside in the outer enamel epithelium (OEE) and underlying stellate reticulum (SR) of

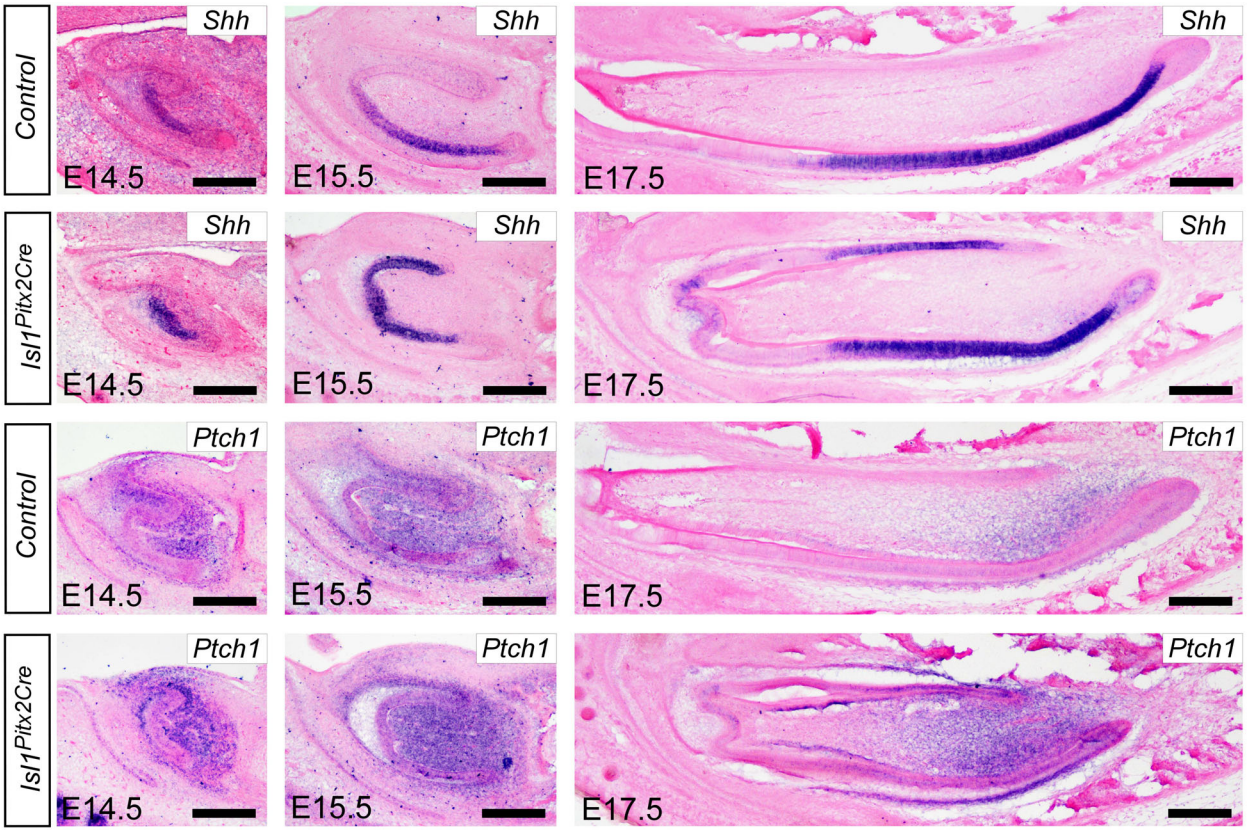

Fig. 7. Expression of *Shh* and *Ptch1* mRNA expression in the incisors of control ($Pitx2^{Cre}$) and $Isl1^{Pitx2Cre}$ at E14.5, E15.5 and E17.5. In situ hybridisation shows the expression of *Shh* in the incisors of control ($Pitx2^{Cre}$) and $Isl1^{Pitx2Cre}$ at E14.5, E15.5 and E17.5 ($n = 3$). The expression of *Ptch1* is detected by in situ hybridisation in incisors of control ($Pitx2^{Cre}$) and $Isl1^{Pitx2Cre}$ at E14.5, E15.5 and E17.5 ($n = 3$). E, embryonic day; scale bars: 200 μm.

laCL [35]. The results suggest that *Isl1* may be critical for the survival of DESCs.

The continuous growth of rodent incisors is achieved by the renewal and differentiation of DESCs [35]. The transcription factor *Sox2*, which is essential for stem cells to maintain pluripotency, has been identified as a specific marker for DESCs [12]. Conditional *Sox2* deletion in the dental epithelium leads to impaired proliferation of DESCs and impaired incisor development [13]. *Sox2* expression was present in both liCL and laCL at cap stage [12]. Subsequently, *Sox2* expression will gradually decrease in the lingual CL. Colocalisation of ISL1 and SOX2 was confirmed in the epithelial cells of incisor. After deletion of *Isl1* with Pitx2-Cre, the expression of SOX2 in liCL and laCL decreased significantly. In particular, SOX2 expression in mutant liCL is absent at E14.5. Our results demonstrate that *Sox2* expression is regulated by *Isl1* in the incisor epithelium. Our previous reports have found that knocking out *Isl1* in palatal epithelial cells also leads to a decrease in *Sox2* expression [36]. The results suggest that *Sox2* is a downstream target gene of *Isl1* in the incisor.

Enamel is the only calcified tissue derived from epithelial cells in mammals. The continuous growing mouse incisor is a good model for studying the spatial and temporal regulation of ameloblast differentiation. The incisor has no lingual enamel due to a lack of ameloblasts on the side [37]. Asymmetric expression patterns of many genes, such as *Shh* and *Fgf3*, are correlated with enamel patterning. *Shh* is strongly expressed in ameloblasts during prosecretory and secretory stages and is a key cell-autonomous factor in ameloblast differentiation [14]. Deletion of *Shh* in dental epithelial cells results in developmental defects of ameloblasts [18]. SHH can induce upregulation of *Amelx* and *Ambn*, the main structural components of enamel, in ameloblasts [18]. Our RNA-seq results also showed that the expression of *Shh* and *Fgf3* was significantly upregulated in the incisors of the mutants. In

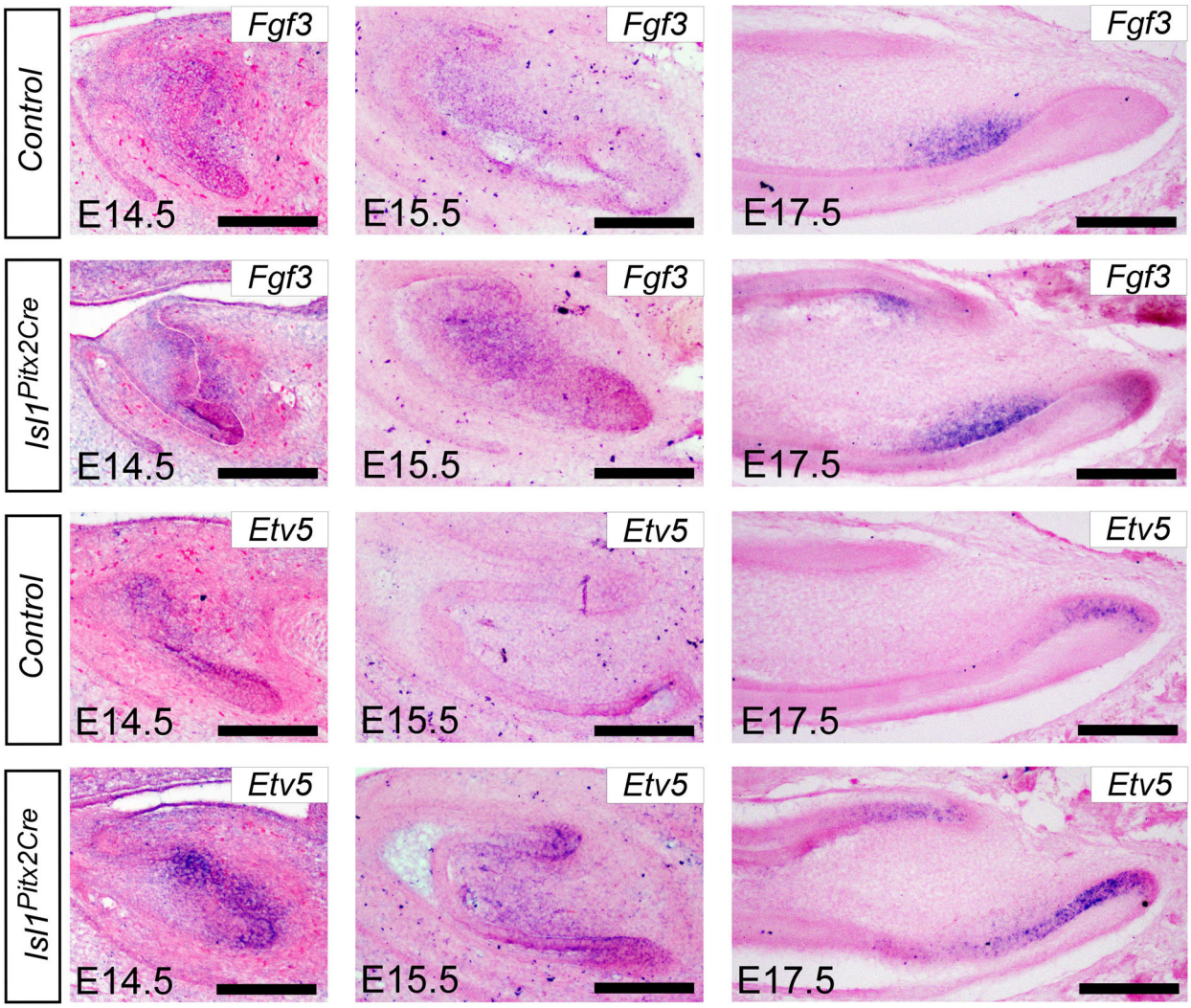

Fig. 8. Expression of *Fgf3* and *Etv5* mRNA expression in the incisors of control ($Pitx2^{Cre}$) and $Isl1^{Pitx2Cre}$ at E14.5, E15.5 and E17.5. In situ hybridisation was performed to detect *Fgf3* and *Etv5* expression in the incisors of control ($Pitx2^{Cre}$) and $Isl1^{Pitx2Cre}$ mice at E14.5, E15.5, and E17.5 ($n = 3$). E, embryonic day; scale bars: 200 μm.

wild-type, *Shh* and *Fgf3* are only detected in labial CL but not lingual CL. Ectopic *Shh* and *Fgf3* expression was found in lingual CL of *Fst* or *Spry4* null mice with ectopic enamel [34,38].

Isl1 is expressed in both labial CL and lingual CL of wild type incisors. Previous studies have shown that conditional knockout of *Isl1* using K14-Cre can also result in ectopic enamel on the lingual surface of the incisor [28]. The phenotype of $Isl1^{Pitx2Cre}$ is much stronger than of $Isl1^{K14Cre}$, and ameloblasts are present on all surfaces of the mutant ($Isl1^{Pitx2Cre}$) incisor. *Shh* and *Fgf3* are upregulated in both labial CL and lingual CL of the mutant ($Isl1^{Pitx2Cre}$) incisor. Furthermore, the *Shh* downstream target genes *Ptch1*, *Fgf3* and *Etv5* were all upregulated in both the labial CL and lingual CL of the mutants ($Isl1^{Pitx2Cre}$). These results indicate that SHH, FGF and BMP signalling activity is upregulated in both the labial CL and lingual CL of the mutants ($Isl1^{Pitx2Cre}$). *Sox2* has been reported to control the asymmetric patterning of ameloblast lineage commitment by regulating SHH and FGF signalling [32], consistent with its inhibitory effect on *Shh* expression in dental epithelial cells [39]. In addition, our published data showed that *Shh* regulate FGF signalling in the incisor [40]. In summary, the early decrease of SOX2 expression in liCL after *Isl1* deletion may lead to the upregulation of SHH, FGF and BMP signalling and the differentiation of lingual epithelial cells.

In summary, our data indicate *Isl1* plays a critical role in asymmetric patterning of ameloblasts and the maintenance of DESCs in the incisors. Deletion of Isl1 leads to significant downregulation of *Sox2* and *Lgr5* (markers of DESCs), resulting in decreased proliferation and increased apoptosis of dental epithelial cells. *Sox2* expression in dental epithelial cells is regulated by *Isl1*, and its downregulation may contribute to ectopic ameloblast differentiation on the lingual side of the incisor.

Materials and methods

Animals

The *Pitx2*-Cre knock-in allele ($Pitx2^{Cre}$) and the ROSA26 Cre reporter strain (*R26R-LacZ*) were obtained from the Mutant Mouse Resource and Research Center (MMRRC_000126-UCD) and The Jackson Laboratory (JAX: 009427), respectively. The *Isl1* conditional knockout allele ($Isl1^{fl}$) and *Isl1-lacZ* knock-in allele ($Isl1^{LacZ}$) were kindly provided by Dr. Lin Gan [22]. All mice were housed at the Laboratory Animal Center of Hangzhou Normal University under sterile conditions, with a 12 h: 12 h light/dark photocycle at 25 ± 1 °C, and had free access to water and food. All experimental protocols involving mice were approved by the Hangzhou Normal University Animal Care and Use Committee (2022–1057). The morning on which a vaginal plug was detected was designated as embryonic day 0.5 (E0.5).

X-gal staining

Whole-mount X-gal staining was performed as described previously [41]. Briefly, after dissection, embryos were fixed in fresh fix buffer (5 mM EGTA, 2 mM MgCl2, and 4% paraformaldehyde (PFA)) for 1 h at 4 °C. Three washes were subsequently performed with a washing buffer (0.02% NP40, 0.01% sodium deoxycholate, and 2 mM MgCl2 in PBS). Embryos were stained with staining buffer (5 mM potassium ferricyanide, 5 mM potassium ferrocyanide, and 0.1% X-gal in washing buffer) for 2–4 h at 37 °C in the dark. The stained embryos were washed with PBS and finally post-fixed in 4% PFA at 4 °C. X-gal stained sections were counterstained with Nuclear Fast Red.

BrdU labelling and TUNEL assays

5-bromodeoxyuridine (BrdU) incorporation was used to analyse cell proliferation [42]. BrdU solution (3 mg/100 g of body weight) was injected intraperitoneally, and embryos were collected 30 min later. Embryonic heads were fixed in 10% neutral buffered formalin at 4 °C overnight and then processed for paraffin sectioning at 5 μm for immunofluorescence staining. Relative cell proliferation was calculated as the percentage of BrdU-positive cells in the mutant compared with controls within a defined arbitrary area. Statistical significance was calculated using Student's *t*-test. Apoptotic cells were detected by TUNEL assay. The In Situ Cell Death Detection kit (Roche, Mannheim, Germany) was used according to the manufacturer's protocol.

Immunofluorescence and histological analysis

Embryos were collected at defined developmental stages and then fixed in 4% PFA for 30 min at 4 °C. The samples were dehydrated in a graded series of 50%, 70%, 80%, 90% and 100% ethanol, cleared with xylene and embedded in paraffin. Sections were stained with haematoxylin and eosin as described previously [43]. Masson's trichrome staining was carried out using a kit (Solarbio life sciences, Beijing, China) following the manufacturer's instructions. For immunofluorescence, sections were washed three times in PBST (0.1% Triton X-100/PBS) and blocked in 5% BSA for 1 h. Subsequently, sections were incubated with primary antibodies overnight in a humid chamber at 4 °C. Primary antibodies used were: BrdU (ab8152; Abcam, Cambridge, MA, USA), SOX2 (66411-1-Ig; Proteintech), ISL1 (ab20670; Abcam), Cleaved Caspase 3 (25128-1-AP; Proteintech, Wuhan, China), Cyclin D1 (A19038; ABclonal, Wuhan, Chin). Secondary antibodies conjugated with Alexa Fluor 488 or 594 (1 : 1000, Invitrogen, Carlsbad, CA, USA) were applied for 1 h in the dark.

In situ hybridisation

In situ hybridisation using a section of embryonic samples was performed as previously described [44]. Embryos were collected at defined developmental stages and fixed in freshly made 4% PFA overnight at 4 °C. Samples were then dehydrated in a graded series of alcohols and embedded in paraffin. After treatment with proteinase K, sections (12 μm) were incubated overnight at 65 °C with a hybridisation solution containing denatured RNA probes. Labelled non-radioactive RNA probes were produced by in vitro transcription using DIG RNA labelling kit (Roche).

RNA-seq analysis and quantitative real-time PCR

RNA-seq was performed using the total RNA extracted from E14.5 mandibular incisors. All the raw data generated from the RNA sequencing (RNA-seq) was deposited in BIGD (GSA: CRA018417) that are publicly accessible at https://ngdc.cncb.ac.cn/gsa. Quantitative real-time PCR was performed in triplicate for each set of samples using a CFX96 Real-Time System (Bio-Rad, Shanghai, China) as previously described [45]. Oligonucleotide primers are as follows: *Shh* (5′-AAAGCTGACCCCTTTAGCCTA and 5′-TGAGTTCCTTAAATCGTTCG GAG), *Ptch1* (5′-AG ACTACCCGAATATCCAGCACC and 5′-CCAGTCAC

TGTCAAATGCATCC), *Gli1* (5′- CCAAGCCAACTTTATCAGGG and 5′- AGCCCGCTTCTTTGTTAATTTGA), *Sox2* (5′- CTTTTGTCCGAGACCGAGAAGC and 5′- CCGGGA AGCGTGTACTTATCC), *Fgf3* (5′- CTTGAGAACAGCGCCTATAGC and 5′- TAGTGATCCGAAGCATACAGC), *Etv4* (5′- ACTAATTGAACCTGAAGAGG and 5′- ACACAAACTTGTACACGTAGC), *Etv5* (5′- CCTGATGATGAGCAGTTTGTCC and 5′- GCACTTTTCTCCATACTTAGCACC), *Lgr5* (5′- CGAGCCTTACAGAGCCTGATACC and 5′- TGTTGCCGTCGTCTTTATTCC), *18S* (5′-TAGAGGGACAAGTGGCGTTC, and 5′-CGCTGAGCCAGTCAGTGT). The relative amount of gene transcript was calculated using the $2^{-\Delta\Delta CT}$ method [46] and normalised to the endogenous *18S* reference gene.

In vitro organ cultures

Incisors were dissected from E14.5 embryos and placed on a Nuclepore Track-Etch membrane (0.2-μm pore size) in TROWELL organ culture in a chemical defined medium as described previously [25]. For *Isl1* overexpression experiments, the *Isl1* overexpression vector (pCDH-Isl1) or control vector (pCDH) was transfected with Lipofectamine3000 reagent. After the explants were cultured for 48 h in a humidified atmosphere of 5% CO_2 at 37 °C, RNA was extracted and real-time quantitative PCR analysis was performed. All experiments were repeated at least three times.

Primary cell culture and luciferase assay

Incisors were carefully dissected from E14.5 wild-type embryos. The explants were incubated in 0.75 $mg{\cdot}mL^{-1}$ Dispase on ice for 30 min. One hundred microliters of isolated primary cells were cultured in 96-well plates. The 3.1 kb promoter of Sox2 was cloned into the pGL3 basic vector to generate pGL3-Sox2 Pro. For the luciferase assay, the pGL3 empty vector (control) or pGL3-Sox2 Pro vector was co-transfected with either the *Isl1* overexpression vector (pCDH-Isl1) or the control vector (pCDH). After 48 h of incubation at 37 °C in a humidified atmosphere containing 5% CO_2, cells were harvested for luciferase activity analysis. Firefly luciferase activities were normalised to *Renilla* luciferase activity and each experiment was performed in triplicate and repeated at least three times.

ChIP assay

For the chromatin immunoprecipitation (ChIP) analysis, incisors were dissected from E14.5 wild type embryos. ChIP was carried out using antibody against ISL1 (Abcam) or normal rabbit IgG (Beyotime, Beijing, China). The eluted DNA served as the template for quantitative real-time PCR (qPCR) analyses, performed in triplicate. The specific primers targeting the predicted ISL1 binding site were as follows: 5′-CTATTATAACCCCAAAAGAGG and 5′-AAGTCTACTGTACTTATCAGAGG.

Statistical analyses

All data are presented as means ± SEM. Student's *t*-test was used to test differences among data sets. *P* values of less than 0.05 were regarded as statistically significant.

Author contributions

FL contributed to conceptualisation; HH, FL contributed to methodology; HH, FL contributed to validation; YQ, HL, YW, SG contributed to data curation; YQ, HL, YW, SG, JL, HH, MQ, FL contributed to data analysis; YQ, HL, YW, SG, FL contributed to investigation; FL contributed to writing – original draft; JL, HH, MQ, FL contributed to writing – review and editing; FL contributed to supervision; FL contributed to project administration; FL contributed to funding acquisition. All authors have read and approved the final version of the manuscript submitted for publication.

Acknowledgements

We thank Dr. Lin Gan for providing $Isl1^{fl}$ and $Isl1^{lacZ}$ mice. This work was supported by Zhejiang Provincial Natural Science Foundation of China (LY24C120002 to FL) and National Natural Science Foundation of China (81871166, 81670971 to FL).

Peer review

The peer review history for this article is available at https://www.webofscience.com/api/gateway/wos/peer-review/10.1111/febs.70713.

Data availability statement

The data supporting the results of this study will be made available upon request.

References

1 Catón J & Tucker AS (2009) Current knowledge of tooth development: patterning and mineralization of the murine dentition. *J Anat* **214**, 502–515.
2 Felszeghy S, Suomalainen M & Thesleff I (2010) Notch signalling is required for the survival of epithelial stem cells in the continuously growing mouse incisor. *Differentiation* **80**, 241–248.

3 Klein OD, Lyons DB, Balooch G, Marshall GW, Basson MA, Peterka M, Boran T, Peterkova R & Martin GR (2008) An FGF signaling loop sustains the generation of differentiated progeny from stem cells in mouse incisors. *Development* **135**, 377–385.
4 Liu F, Dangaria S, Andl T, Zhang Y, Wright AC, Damek-Poprawa M, Piccolo S, Nagy A, Taketo MM, Diekwisch TGH *et al.* (2010) β-catenin initiates tooth neogenesis in adult rodent incisors. *J Dent Res* **89**, 909–914.
5 Seidel K, Ahn CP, Lyons D, Nee A, Ting K, Brownell I, Cao T, Carano RAD, Curran T, Schober M *et al.* (2010) Hedgehog signaling regulates the generation of ameloblast progenitors in the continuously growing mouse incisor. *Development* **137**, 3753–3761.
6 Volckaert T, Yuan TT, Chao CM, Bell H, Sitaula A, Szimmtenings L, El Agha E, Chanda D, Majka S, Bellusci S *et al.* (2017) Fgf10-hippo epithelial-mesenchymal crosstalk maintains and recruits lung basal stem cells. *Dev Cell* **43**, 48–59.
7 Wang XP, Suomalainen M, Felszeghy S, Zelarayan LC, Alonso MT, Plikus MV, Maas RL, Chuong CM, Schimmang T & Thesleff I (2007) An integrated gene regulatory network controls stem cell proliferation in teeth. *PLoS Biol* **5**, 1324–1333.
8 Balic A (2019) Concise review: cellular and molecular mechanisms regulation of tooth initiation. *Stem Cells* **37**, 26–32.
9 Biggs LC & Mikkola ML (2014) Early inductive events in ectodermal appendage morphogenesis. *Semin Cell Dev Biol* **25**, 11–21.
10 Thesleff I, Wang XP & Suomalainen M (2007) Regulation of epithelial stem cells in tooth regeneration. *C R Biol* **330**, 561–564.
11 Gan L, Liu Y, Cui DX, Pan Y & Wan M (2020) New insight into dental epithelial stem cells: identification, regulation, and function in tooth homeostasis and repair. *World J Stem Cells* **12**, 1327–1340.
12 Juuri E, Saito K, Ahtiainen L, Seidel K, Tummers M, Hochedlinger K, Klein OD, Thesleff I & Michon F (2012) Sox2+ stem cells contribute to all epithelial lineages of the tooth via Sfrp5+ progenitors. *Dev Cell* **23**, 317–328.
13 Sanz-Navarro M, Seidel K, Sun Z, Bertonnier-Brouty L, Amendt BA, Klein OD & Michon F (2018) Plasticity within the niche ensures the maintenance of a stem cell population in the mouse incisor. *Development* **145**, dev155929.
14 Takahashi S, Kawashima N, Sakamoto K, Nakata A, Kameda T, Sugiyama T, Katsube KI & Suda H (2007) Differentiation of an ameloblast-lineage cell line (ALC) is induced by sonic hedgehog signaling. *Biochem Biophys Res Commun* **353**, 405–411.
15 Zhang L, Hua F, Yuan GH, Zhang YD & Chen Z (2008) Sonic hedgehog signaling is critical for cytodifferentiation and cusp formation in developing mouse molars. *J Mol Histol* **39**, 87–94.
16 Du W, Du W & Yu HY (2018) The role of fibroblast growth factors in tooth development and incisor renewal. *Stem Cells Int* **2018**, 7549160.
17 Cobourne MT, Xavier GM, Depew M, Hagan L, Sealby J, Webster Z & Sharpe PT (2009) Sonic hedgehog signalling inhibits palatogenesis and arrests tooth development in a mouse model of the nevoid basal cell carcinoma syndrome. *Dev Biol* **331**, 38–49.
18 Dassule HR, Lewis P, Bei M, Maas R & McMahon AP (2000) Sonic hedgehog regulates growth and morphogenesis of the tooth. *Development* **127**, 4775–4785.
19 Gritli-Linde A, Bei M, Maas R, Zhang XM, Linde A & McMahon AP (2002) Shh signaling within the dental epithelium is necessary for cell proliferation, growth and polarization. *Development* **129**, 5323–5337.
20 Kettunen P, Spencer-Dene B, Furmanek T, Kvinnsland IH, Dickson C, Thesleff I & Luukko K (2007) Fgfr2b mediated epithelial-mesenchymal interactions coordinate tooth morphogenesis and dental trigeminal axon patterning. *Mech Dev* **124**, 868–883.
21 Kim E, Jiang M, Huang HC, Zhang YC, Tjota N, Gao X, Robert J, Gilmore N, Gan L & Que JW (2019) Isl1 regulation of Nkx2.1 in the early foregut epithelium is required for trachea-esophageal separation and lung Lobation. *Dev Cell* **51**, 675–683.
22 Pan L, Deng M, Xie XL & Gan L (2008) ISL1 and BRN3B co-regulate the differentiation of murine retinal ganglion cells. *Development* **135**, 1981–1990.
23 Li FX, Fu GQ, Liu Y, Miao XP, Li Y, Yang XQ, Zhang XY, Yu DL, Gan L, Qiu MS *et al.* (2017) ISLET1-dependent β-catenin/hedgehog signaling is required for outgrowth of the lower jaw. *Mol Cell Biol* **37**, e00590-16.
24 Mitsiadis TA, Angeli I, James C, Lendahl U & Sharpe PT (2003) Role of Islet1 in the patterning of murine dentition. *Development* **130**, 4451–4460.
25 Zhang W, Yu JJ, Fu GQ, Li JY, Huang HR, Liu J, Yu DL, Qiu MS & Li FX (2022) ISL1/SHH/CXCL12 signaling regulates myogenic cell migration during mouse tongue development. *Development* **149**, dev200788.
26 Moretti A, Caron L, Nakano A, Lam JT, Bernshausen A, Chen YH, Qyang YB, Bu L, Sasaki M, Martin-Puig S *et al.* (2006) Multipotent embryonic isl1+ progenitor cells lead to cardiac, smooth muscle, and endothelial cell diversification. *Cell* **127**, 1151–1165.
27 Bu L, Jiang X, Martin-Puig S, Caron L, Zhu SJ, Shao Y, Roberts DJ, Huang PL, Domian IJ & Chien KR (2009) Human ISL1 heart progenitors generate diverse multipotent cardiovascular cell lineages. *Nature* **460**, 113–117.

28 Naveau A, Zhang B, Meng B, Sutherland MT, Prochazkova M, Wen T, Marangoni P, Jones KB, Cox TC, Ganss B *et al.* (2017) Isl1 controls patterning and mineralization of enamel in the continuously renewing mouse incisor. *J Bone Miner Res* **32**, 2219–2231.
29 Liu W, Selever J, Lu MF & Martin JF (2003) Genetic dissection of Pitx2 in craniofacial development uncovers new functions in branchial arch morphogenesis, late aspects of tooth morphogenesis and cell migration. *Development* **130**, 6375–6385.
30 Bei M (2009) Molecular genetics of ameloblast cell lineage. *J Exp Zool Part B* **312b**, 437–444.
31 Suomalainen M & Thesleff I (2010) Patterns of Wnt pathway activity in the mouse incisor indicate absence of Wnt/β-catenin signaling in the epithelial stem cells. *Dev Dyn* **239**, 364–372.
32 Li D, Wang XF, Yao LP, Jing HX, Qin TT, Li MY, Zhang SY, Chen Z & Zhang L (2021) Sox2 controls asymmetric patterning of ameloblast lineage commitment by regulation of FGF signaling in the mouse incisor. *J Mol Histol* **52**, 1035–1042.
33 Kyrylkova K, Kyryachenko S, Biehs B, Klein O, Kioussi C & Leid M (2012) BCL11B regulates epithelial proliferation and asymmetric development of the mouse mandibular incisor. *PLoS One* **7**, e37670.
34 Boran T, Peterkova R, Lesot H, Lyons DB, Peterka M & Klein OD (2009) Temporal analysis of ectopic enamel production in incisors from Sprouty mutant mice. *J Exp Zool Part B* **312b**, 473–485.
35 Yu T, Volponi AA, Babb R, An ZW & Sharpe PT (2015) Stem cells in tooth development, growth, repair, and regeneration. *Craniofacial Development* **115**, 187–212.
36 Zhang CJ, Zheng YT, Qu YP, Huang RQ, Huang HR, Li JY, Qiu MS & Li FX (2025) Transcriptional factor ISL1 regulates palate development by tuning the SHH cascad. *FEBS J* **292**, 851–863.
37 Smith CE & Warshawsky H (1975) Histological and three dimensional organization of the odontogenic organ in the lower incisor of 100 gram rats. *Am J Anat* **142**, 403–429.
38 Wang XP, Suomalainen M, Jorgez CJ, Matzuk MM, Werner S & Thesleff I (2004) Follistatin regulates enamel patterning in mouse incisors by asymmetrically inhibiting BMP signaling and ameloblast differentiation. *Dev Cell* **7**, 719–730.
39 Sun Z, Yu WJ, Navarro MS, Sweat M, Eliason S, Sharp T, Liu H, Seidel K, Zhang L, Moreno M *et al.* (2016) Sox2 and Lef-1 interact with Pitx2 to regulate incisor development and stem cell renewal. *Development* **143**, 4115–4126.
40 Zheng Y, Qu Y, Liu H, Huang H, Li J, Qiu M & Li F (2025) Epithelial YAP1 regulates ameloblast differentiation through SHH/FGF signaling. *J Dent Res*, 220345251336164 doi: 10.1177/00220345251336164
41 Huang RQ, Zhang CJ, Zheng YT, Zhang W, Huang HR, Qiu MS, Li JY & Li FX (2023) ISL1 regulates lung branching morphogenesis via Shh signaling pathway. *J Biol Chem* **299**, 105034.
42 Huang HR, Yang XJ, Bao ML, Cao HH, Miao XP, Zhang XY, Gan L, Qiu MS & Zhang ZY (2016) Ablation of the Sox11 gene results in Clefting of the secondary palate resembling the Pierre Robin sequence. *J Biol Chem* **291**, 7107–7118.
43 Chen LY, Zhang W, Huang RQ, Miao XP, Li JY, Yu DL, Li Y, Hsu W, Qiu MS, Zhang ZY *et al.* (2021) The function of Wls in ovarian development. *Mol Cell Endocrinol* **522**, 111142.
44 Li J, Xu J, Cui Y, Wang L, Wang B, Wang Q, Zhang X, Qiu M & Zhang Z (2019) Mesenchymal Sufu regulates development of mandibular molar via Shh signaling. *J Dent Res* **98**, 1348–1356.
45 Li FX, Ma HH & Liu J (2018) Pyrethroid insecticide Cypermethrin modulates gonadotropin synthesis via calcium homeostasis and ERK1/2 signaling in LβT2 mouse pituitary cells. *Toxicol Sci* **162**, 43–52.
46 Livak KJ & Schmittgen TD (2001) Analysis of relative gene expression data using real-time quantitative PCR and the 2(-Delta Delta C(T)) method. *Methods* **25**, 402–408.

